Separation Science and Technology
Publication details, including instructions for authors and subscription information:
http://www.informaworld.com/smpp/title~content=t713708471

The Combined Effect of Diffusion and Evaporation on the Molecular Distillation of Ideal Binary Liquid Mixtures

E. Ruckenstein[ab]; W. J. Hassink[a]; Sathya Murthy V. Gourisankar[c]
[a] DEPARTMENT OF CHEMICAL ENGINEERING, UNIVERSITY OF DELAWARE, NEWARK, DELAWARE [b] Department of Chemical Engineering, State University of New York at Buffalo, Buffalo, New York [c] DEPARTMENT OF CHEMICAL ENGINEERING, STATE UNIVERSITY OF NEW YORK AT BUFFALO, BUFFALO, NEW YORK

To cite this Article Ruckenstein, E. , Hassink, W. J. and Gourisankar, Sathya Murthy V.(1983) 'The Combined Effect of Diffusion and Evaporation on the Molecular Distillation of Ideal Binary Liquid Mixtures', Separation Science and Technology, 18: 6, 523 — 545
To link to this Article: DOI: 10.1080/01496398308060292
URL: http://dx.doi.org/10.1080/01496398308060292

SEPARATION SCIENCE AND TECHNOLOGY, 18(6), pp. 523-545, 1983

The Combined Effect of Diffusion and Evaporation on the Molecular Distillation of Ideal Binary Liquid Mixtures

E. RUCKENSTEIN* and W. J. HASSINK

DEPARTMENT OF CHEMICAL ENGINEERING
UNIVERSITY OF DELAWARE
NEWARK, DELAWARE 19711

SATHYA MURTHY V. GOURISANKAR

DEPARTMENT OF CHEMICAL ENGINEERING
STATE UNIVERSITY OF NEW YORK AT BUFFALO
BUFFALO, NEW YORK 14260

Abstract

A treatment which takes into account the effects of both diffusion in the liquid film and evaporation on the rate of molecular distillation of binary liquid mixtures in the falling film and rotary cone stills has been developed. The conditions under which the rate of molecular distillation in these stills is determined by either evaporation alone or evaporation together with diffusion have been identified. The interface temperature, film thickness, and concentration profiles were obtained by a numerical solution of the system equations for both cases. For the falling film stills, the limiting case of an evaporation rate controlled process was approached when, at the inlet of the still, the ratio $E_I = k_1\delta_0/D$ was less than 0.1 for all the ratios $K_I = k_2/k_1$ greater than 0.086, where k_1 and k_2 are the evaporation rate coefficients of the more and less volatile components of the mixture, respectively, D is the diffusion coefficient of the more volatile component, δ_0 is the initial film thickness, and the subscript I refers to the conditions at the liquid film surface. For $k_2/k_1 > 0.4$, the above approximation was still satisfactory for all values of $E_I < 1.5$. The rotary cone stills were found not to be affected by diffusion in the liquid film and, therefore, well represented by the evaporation rate controlling mechanism over the full range of distillation parameters investigated.

*To whom correspondence should be addressed at the following present address: Department of Chemical Engineering, State University of New York at Buffalo, Buffalo, New York 14260.

 0149-6395/83/1806-0523$3.50/0

INTRODUCTION

Molecular distillation belongs to the category of high vacuum distillation techniques, with the distinct feature that the vapor path is unobstructed and the condenser is separated from the evaporator by a distance less than the mean free path of the evaporating molecules. This technique finds application in the separation and purification of high molecular weight, thermally sensitive materials whose volatilities are too low to permit conventional distillation.

In this special form of evaporative distillation the distance between the evaporator and condenser is typically in the range of 1 to 20 cm, being more usually in the range of 1 to 5 cm. The pressure above the liquid surface is below 10^{-3} torr and may be as low as 5×10^{-5} torr in a soundly constructed molecular distillation apparatus. Under these conditions the mean free path of the molecules is larger than the distance between the evaporator and condenser. Consequently, there is practically no return of molecules from the gas to the liquid phase and the rate of distillation is solely governed by the rate of molecular escape from the liquid surface. Therefore, in molecular distillation there is neither an equilibrium between the liquid and vapor nor is there any effect of vapor space conditions on the rate of distillation, features which differentiate it from both differential distillation and evaporative distillation, respectively.

The evolution of molecular still design witnessed the transition from "pot stills" to "falling film" and "rotary cone" stills, the developments arising primarily from efforts to decrease both the distillation temperature and the time of exposure of the distilland.

During the molecular distillation of binary liquid mixtures in the falling film and rotary cone stills, the distilland flows as a thin liquid film over a heated evaporator surface, under the action of gravitational and centrifugal forces, respectively. Due to the higher evaporation rate of the more volatile component of the liquid mixture, surface depletion of this species takes place in comparison to the bulk of the liquid, giving rise to concentration gradients of both the components in opposite directions within the liquid film. Under these conditions, the usual assumption involved in the theoretical treatments of the early molecular stills (pot stills), namely, that the distilland is well-mixed, is no longer valid. Therefore, in the analyses of the falling film and rotary cone stills, the effects of both diffusion and evaporation on the rate of molecular distillation need to be considered.

Greenberg (*4*) has given a quantitative picture of the variables affecting high vacuum, molecular distillation in centrifugal stills. He considered molecular distillation to be a surface phenomenon, with evaporation solely

influencing the rate of the process. This assumption seems well suited to centrifugal stills, where the film thicknesses are small (of the order of 5×10^{-3} cm) and, therefore, diffusional resistances in the liquid films are insignificant. In the case of the falling film stills, however, larger film thicknesses are encountered (0.01 to 0.3 cm), necessitating the consideration of the effects of both diffusion and evaporation on the still performance.

This work investigates the effect of diffusion within the liquid film and its interaction with evaporation on the performance of both the falling film and rotary cone stills during the molecular distillation of ideal binary liquid mixtures. An effort has been made to delineate quantitatively the conditions under which either evaporation alone or evaporation together with diffusion affects the rate of the process.

RATE OF VAPORIZATION

An expression for the molar evaporation rate of a pure liquid is available from the kinetic theory of gases as follows (*6*):

$$N = P\left(\frac{1}{2\pi TMR_g}\right)^{1/2} \tag{1}$$

An evaporation coefficient, α, is used to account for the decrease in the observed evaporation rate from that of the theoretical one predicted by Eq. (*1*). The physical significance of α has been the subject of numerous investigations (*1, 2, 5, 7, 8*). Greenberg (*4*) provides a compilation of experimental and theoretically calculated evaporation coefficients for a number of common compounds.

In this treatment the evaporation coefficient α is absorbed into the evaporation rate coefficient k and assumed to be a constant for the specific system under investigation. The modified version of Eq. (1), written for each component of an ideal binary liquid mixture, is given by

$$N = \frac{c_i}{c_T}\alpha_i P_i\left(\frac{1}{2\pi R_g TM_i}\right)^{1/2} = k_i c_i \tag{2}$$

where P_i is the vapor pressure, k_i is the evaporation rate coefficient, and c_i is the molar concentration of component i, respectively, and c_T is the total molar concentration of the mixture. Component 1 is considered to be the more volatile component of the liquid mixture.

FALLING FILM STILL

In the falling film still, the liquid mixture flows as a thin film under the action of gravity over a heated evaporator surface. A condenser in close proximity to the evaporator (closer than the mean free path of the distilling molecules) and a low pressure atmosphere in the system (less than 10^{-3} torr), provide the means for the molecular distillation of the binary liquid mixture.

An analysis of the coupled phenomena of fluid dynamics, heat transfer, mass transfer, and surface evaporation will provide a system of equations for the film thickness, concentration, and temperature profiles in the falling film stills. The development of these equations is outlined below.

Velocity Profile

The liquid film flows down the evaporator surface which is generally either cylindrical or planar. When the film thickness is small compared to the evaporator radius of curvature, i.e., $\delta/R \ll 1$, the film flow can be approximated as for a planar surface. This is the situation under investigation.

The velocity profile for the laminar, steady flow of a Newtonian fluid in a falling film was derived by Nusselt to be

$$u = \frac{g\delta^2}{\nu}\left\{\frac{y}{\delta} - \frac{1}{2}\left(\frac{y}{\delta}\right)^2\right\} \tag{3}$$

where u is the axial component of the film velocity, y is the distance from the evaporator surface, ν is the kinematic viscosity, g is the gravitational acceleration, and δ is the film thickness.

The normal component of the film velocity, v, derived using the continuity equation, the noslip condition at the evaporator surface and Eq. (3), has the form

$$v = -\frac{gy^2}{2\nu}\frac{d\delta}{dx} \tag{4}$$

Film Thickness Profile

The liquid film thickness decreases axially due to evaporation of both components of the film. The change in the axial flux of each component is

equal to the amount of that component vaporized over the incremental axial distance, i.e.,

$$\frac{d}{dx}\int_0^{\delta} uc_i\, dy = -k_i c_{il} \tag{5}$$

Assuming the total molar concentration of the liquid mixture ($c_1 + c_2 = c_T$) to be constant and using the axial velocity profile (Eq. 3), a relation for the film thickness profile may be derived as

$$\frac{g\delta^2}{\nu}\frac{d\delta}{dx} = -\left\{(k_1 - k_2)\left(\frac{c_{1,I}}{c_T}\right) + k_2\right\} \tag{6}$$

with the boundary condition

$$\delta = \delta_0 \text{ at } x = x_0 \tag{7}$$

Concentration Profile

Neglecting diffusion in the axial direction, the convective diffusion equation reduces to the following form for Component 1:

$$u\frac{\partial c_1}{\partial x} + v\frac{\partial c_1}{\partial y} = D\frac{\partial^2 c_1}{\partial y^2} \tag{8}$$

where D is the diffusion coefficient, assumed to be independent of concentration. Two of the boundary conditions are

$$c_1 = c_0 \text{ at } x = 0,\ 0 \le y \le \delta \tag{9}$$

$$\frac{\partial c_1}{\partial y} = 0 \text{ at } y = 0,\ x \ge 0 \tag{10}$$

The third boundary condition is derived in the following manner. The continuity equation is combined with the convective diffusion equation, the latter integrated across the film, and then rearranged using the noslip condition at the evaporator surface together with Eq. (10), to the following form:

$$\int_0^{\delta} \frac{\partial(uc_1)}{\partial x}\, dy + (vc_1)_I = D\left(\frac{\partial c_1}{\partial y}\right)_I \tag{11}$$

The integral in Eq. (11) can be rewritten using Leibnitz's formula:

$$\frac{d}{dx}\int_0^{\delta} (uc_1)\, dy = (uc_1)_I \frac{d\delta}{dx} + \int_0^{\delta} \frac{\partial(uc_1)}{\partial x}\, dy \tag{12}$$

Substituting Eq. (12) in Eq. (11) and using the known expressions for the film velocity components and evaporation rates, one obtains

$$-D\left(\frac{\partial c_1}{\partial x}\right)_I - \frac{g\delta^2 c_{1,I}}{\nu}\frac{d\delta}{dx} = k_1 c_{1,I} \tag{13}$$

Equation (13) equates the rate of vaporization of Component 1 from the film to its convective and diffusive transport to the film surface. It provides the third boundary condition for the film concentration profile.

Temperature Profile

The calculation of the temperature profile is carried out with the simplifying assumptions that convective heat transfer is negligible compared to conductive heat transfer and the feed is at its distillation temperature.

The energy conservation equation, when the above approximations are used, takes the form

$$q = \frac{T_W - T_I}{\delta}\theta = k_1 c_{1,I}\Delta h_1 + k_2 c_{2,I}\Delta h_2 + \sigma(T_I^4 - T_C^4) \tag{14}$$

where σ is the Stefan Boltzman constant, T_W is the temperature in °K at the wall, T_I is the temperature at the free interface, T_C is the temperature of the condenser, and Δh_1 and Δh_2 are the heats of vaporization of the two components.

The heating involves either a condensing vapor or some form of electrical heating. Consequently, it may be treated either assuming a constant evaporator temperature or a constant heat input source.

The distilland surface temperature is not constant because of the variations in the film thickness and component concentrations over the length of the

film. To relate the evaporation rate to temperature, a relation between the vapor pressure and temperature of the following form is used:

$$\ln (P_i) = a_i - \frac{b_i}{T_I} \tag{15}$$

The evaporation rate coefficient can now be written as

$$k_i = \frac{e^{(a_i - b_i/T_I)}}{c_T} \left(\frac{1}{2\pi M_i R_g T_I} \right)^{1/2} \tag{16}$$

where the evaporation coefficient (α_i) is taken to be unity.

The complete system of equations describing the falling film still can be written in nondimensional form as below.

Film Thickness Profile

$$\Lambda^2 \frac{d\Lambda}{dX} = -E_I((1 - K_I)C_I + K_I) \tag{17}$$

with the boundary condition

$$\Lambda = 1 \text{ at } X = 0 \tag{18}$$

where $\Lambda = \delta/\delta_0$, $X = x\nu D/g\delta_0^4$, $E_I = k_1\delta_0/D$, $K_I = k_2/k_1$, and $C = c_1/c_T$. The dimensionless parameter, E_I, which contains the ratio of the rates of evaporation to diffusion, provides a measure of the relative importance of the two phenomena on the rate of the process.

Concentration Profile

$$\Lambda^2 \left\{ \frac{Y}{\Lambda} - \frac{1}{2}\frac{Y^2}{\Lambda^2} \right\} \frac{\partial C}{\partial X} - \frac{Y^2}{2}\frac{d\Lambda}{dX}\frac{\partial C}{\partial Y} = \frac{\partial^2 C}{\partial Y^2} \tag{19}$$

with the boundary conditions:

$$C = C_0 \text{ at } X = 0 \tag{20}$$

$$\partial C/\partial Y = 0 \text{ at } Y = 0 \tag{21}$$

and

$$\frac{\partial C}{\partial Y} = -E_I C_I - \Lambda^2 \left(\frac{d\Lambda}{dX}\right) C_I \text{ at } Y = \frac{\delta}{\delta_0} \tag{22}$$

Temperature Profile

Constant Evaporator Heat Flux

$$T'_I = \left\{\frac{(Q - E_I C_I - K_I H' E_1 (1 - C_I))}{\varepsilon} + (T'_C)^4\right\}^{1/4} \tag{23}$$

where $T' = T/T_0$, $Q = q\delta_0/DC_T\Delta h_1$, $H' = \Delta h_2/\Delta h_1$, and $\varepsilon = \sigma\delta_0 T_0^4/DC_T\Delta h_1$.

Constant Evaporator Temperature

$$T'_I = 1 - \Lambda\{H' K_I E_I H + C_I E_I X(1 - H' K_I) + \gamma((T'_I)^4 - (T'_C)^4\} \tag{24}$$

where $T' = T/T_W$, $\gamma = \sigma\delta_0 T_W^3/\theta$, and $H = DC_T\Delta h_1/\theta T_W$.

In these equations,

$$E_I = E_0(T'_I)^{1/2} e^{A(1 - 1/T'_I)} \tag{25}$$

and

$$K_I = K_0 e^{A(1 - 1/T'_I)(B - 1)} \tag{26}$$

The coupled set of Eqs. (17) through (26) can only be solved numerically. In certain limiting cases, however, they can be simplified.

Falling Film Still—Evaporation Rate Controlling Case

When the rate of evaporation controls the distillation process ($D \gg k_1\delta$), the concentration variation of components in the y direction can be

neglected. In other words,

$$C_I = C = f(X) \tag{27}$$

In this limiting case the above equations become:

Film Thickness Profile

$$\Lambda^2 \frac{d\Lambda}{dX} = -E_I\{(1 - K_I)C + K_I\} \tag{28}$$

with

$$\Lambda = 1 \text{ at } X = 0 \tag{29}$$

Concentration Profile

$$C = C_0 \exp\left\{-\int_0^X \left(\frac{3}{\Lambda}\right)\left(\frac{d\Lambda}{dX} + \frac{E_1}{\Lambda^2}\right) dX\right\} \tag{30}$$

Temperature Profile

Equations (23) and (24) are unaltered for this case. Although more simple than the previous one, the above set of equations still requires a numerical solution.

The final results for the falling film still are reported in terms of the reduced average distilland composition C_r, the reduced film flow rate f_r, and the reduced distillate composition C_d, defined as follows:

$$C_r = \left\{\int_0^\delta uC\, dy \Big/ \int_0^\delta u\, dy\right\}/C_0 \equiv \frac{3}{\Lambda^2}\int_0^\Lambda \left(Y - \frac{Y^2}{2\Lambda}\right)\frac{C}{C_0}\, dY \tag{31}$$

$$f_r = \int_0^\delta u\, dy \Big/ \int_0^{\delta_0} u_0\, dy = \Lambda^3 \tag{32}$$

and

$$C_d = C_0(1 - C_r f_r)/(1 - f_r) \tag{33}$$

ROTARY CONE STILL

Due to the greater accelerations occurring in the rotary cone stills in comparison to the falling film stills (centrifugal versus gravitational, respectively), very thin liquid films of the order of 0.005–0.05 mm, flowing rapidly along the surface, are encountered in the former. Because of this, the exposure time of the distilland is reduced in the rotary cone stills, therefore enabling them to process highly thermal sensitive materials.

As in the falling film stills, a treatment which includes the effects of both diffusion and evaporation in these stills is developed along the following lines.

Velocity Profile

If the Coriolis acceleration is neglected and the film thickness is considered small enough for the flow to be laminar, the expression originally derived by Emslie (*3*) can be used to describe the velocity on a rapidly rotating truncated cone:

$$u = \frac{(\omega \sin \phi)^2 x}{\nu} \left(\delta y - \frac{y^2}{2} \right) \tag{34}$$

where the coordinate axes are shown in Fig. 1.

The equations for the film thickness, concentration, and temperature profiles of the rotary cone stills can be derived along the same lines as for the falling film stills, using Eq. (34) for the velocity along the x axis and taking into account the change in area as the liquid film spreads radially along the cone. The nondimensional equations describing the rotary cone stills are as follows:

Film Thickness Profile

$$\frac{d\Lambda}{d\bar{X}} = -\frac{2}{3}\left(\frac{\Lambda}{\bar{X}}\right) - \frac{E_I(C_I(1 - K_I) + K_I)}{W\Lambda^2\bar{X}} \tag{35}$$

with

$$\Lambda = 1 \text{ at } \bar{X} = 1 \tag{36}$$

where $\bar{X} = x/x_0$ and $W = \omega^2 \delta_0^2 \sin^2 \phi / \nu D$.

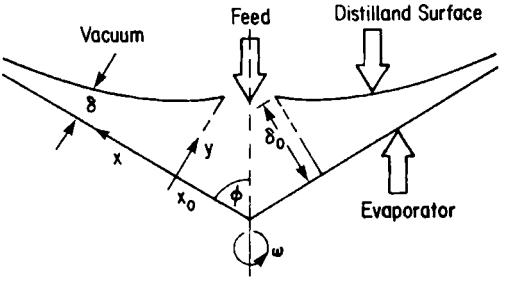

FIG. 1. Coordinate system for the rotary cone still.

Concentration Profile

$$W\bar{X}\left(\Lambda Y - \frac{Y^2}{2}\right)\frac{\partial C}{\partial \bar{X}} + \frac{WY^2}{2}\left\{\frac{2Y}{3} - 2\Lambda - \bar{X}\frac{d\Lambda}{d\bar{X}}\right\}\frac{\partial C}{\partial Y} = \frac{\partial^2 C}{\partial Y^2} \tag{37}$$

with

$$C = C_0 \text{ at } \bar{X} = 1 \tag{38}$$

$$\partial C/\partial Y = 0 \text{ at } Y = 0 \tag{39}$$

and

$$\left(\frac{\partial C}{\partial Y}\right)_I = -C_I\left\{E_I + \frac{W}{3}\left(2\Lambda^3 + 3\Lambda^2\bar{X}\frac{d\Lambda}{d\bar{X}}\right)\right\} \tag{40}$$

Temperature Profile

Equations (23) and (24) remain valid for this case also.

Rotary Cone Still—Evaporation Rate Controlling Case

As for the falling film stills, in this limiting case $C_1 = C_{1,I}$ for any x position. The equations reduce in this limiting case to the following expressions:

Film Thickness Profile

$$\frac{d\Lambda}{d\bar{X}} = -\frac{2}{3}\frac{\Lambda}{\bar{X}} - \frac{E_l(C(1-K_l)+K_l)}{\bar{X}W\Lambda^2} \tag{41}$$

with

$$\Lambda = 1 \text{ at } \bar{X} = 1 \tag{42}$$

Concentration Profile

$$C = C_0 \exp - \int_1^x \left(\frac{2}{\bar{X}} + \frac{3}{\Lambda}\frac{d\Lambda}{d\bar{X}} + \frac{3E_l}{\bar{X}W\Lambda^3}\right) d\bar{X} \tag{43}$$

Temperature Profile

Equations (23) and (24) remain applicable to this case.

The final results are expressed in terms of the reduced variables as for the falling film stills. The expressions for the reduced distilland composition (C_r) and reduced distillate composition (C_d) remain unchanged (Eqs. 31 and 33), while that for the reduced flow rate changes to

$$f_r = (\Lambda^3)\bar{X}^2 \tag{44}$$

SOLUTION OF THE FALLING FILM AND ROTARY CONE STILL EQUATIONS

The implicit system of equations describing the film thickness, concentration, and temperature profiles of the falling film and rotary cone stills can only be solved numerically. The approach adopted in solving these equations is to superimpose a grid network on the liquid film and solve simultaneously for the film thickness, concentration, and temperature profiles, making use of the finite difference technique. The computational scheme for both the falling film and rotary cone stills proceeded as follows: At a particular value of x, the interface temperature was first calculated, followed by an estimate of the ratios E_l and K_l. Then the film thickness and concentrations were evaluated at that value of x. After obtaining convergence of all calculated values, the procedure was repeated for other values of x to obtain the film thickness,

TABLE 1
Values of Physical Properties Used in the Computations

No.	Quantity	Value
1	Molecular weight	300–1200
2	Heat of vaporization	20,000–40,000, cal/g·mol
3	Concentration (C_1, C_2)	7.5×10^4 g·mol/cc
4	Kinematic viscosity	0.35 cm^2/s at 500 K
5	Evaporation rate coefficient of Component 1 at 500 K	0.4 cm/s
6	Diffusion coefficient of Component 1 at 500 K	4×10^{-3} cm^2/s
7	Thermal conductivity	4×10^{-4} cal/cm·s·K

concentration, and temperature profiles. The values of the physical properties used in the computations, assuming a distillation temperature of 500 K, are listed in Table 1.

RESULTS AND DISCUSSION

Falling Film Stills

Figure 2 shows the axial film thickness profile for two different initial concentrations of the feed mixture. Based on the profile of Fig. 2, the concentration profiles will be reported in terms of Λ in the remaining plots. It is important to note that while Λ varies between 1 and 0.8, x varies between zero and several hundred centimeters, depending on the value of E_0.

The dimensionless parameters E_I and K_I, which represent the ratios of the rates of evaporation to diffusion and evaporation rate coefficients, respectively, have a significant bearing on the still performance. Figure 3 shows the effect of E_0 ($= (k_1 \delta_0 / D)_0$) on the surface depletion of Component 1 (lighter component) for $K_0 = 0.1$. The profiles show that, at each value of E_0, the surface depletion of Component 1 initially increases, reaches a maximum, and then decreases with decreasing film thickness. This is due to the influence of two opposing effects when the film thickness decreases axially; namely, (a) lower film diffusional resistance and (b) increased component evaporation rates due to the increase in the film interface temperature. When the component evaporation rates are high enough to offset the effect of lower film thicknesses (lower diffusional resistance), increasing surface depletion of the lighter component takes place, as seen in the initial axial section of the still. After a certain axial distance, however, the rate of diffusion becomes

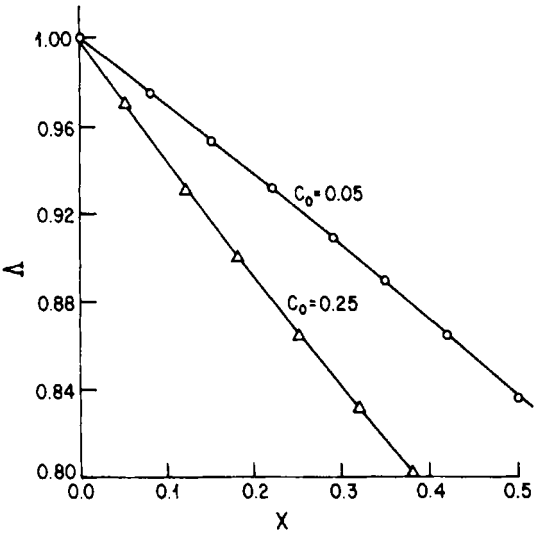

FIG. 2. Axial film thickness profile for two different initial concentrations of the feed mixture for the falling film stills. The following values of the dimensionless parameters were used for this profile: $E_0 = 5.0$, $A = 15.0$, $H = 0.07$, $K_0 = 0.1$, $B = H' = 1.5$, $\gamma = 0.008$, and $T_C = 0.5$.

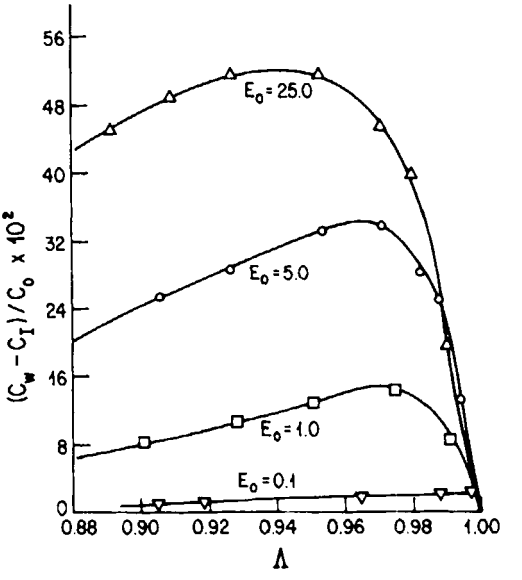

FIG. 3. Ratio of concentration difference across the film to initial concentration of Component 1 versus Λ for various values of E_0 in falling film stills. The other parameters used for this plot are the same as in Fig. 2, except that C_0 is maintained at 0.25 in this figure.

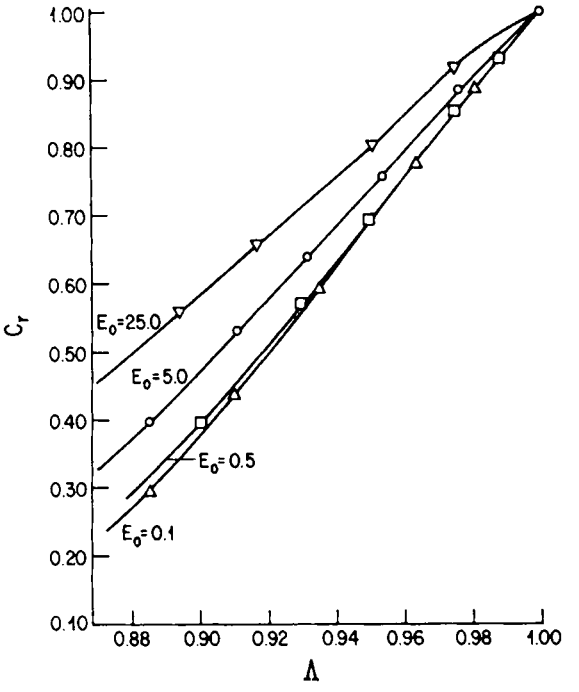

FIG. 4. Reduced film concentration of Component 1 (Eq. 31) versus Λ for varying values of E_0 in falling film stills, with the same values of the other parameters as in Fig. 3.

more comparable to the rate of vaporization, giving rise to decreasing surface depletion of Component 1, as seen in the profiles of Fig. 3. It can be seen from this figure that, as E_0 decreases, the surface depletion of Component 1 becomes less severe and at $K_0 = 0.1$, if $E_0 \leq 0.1$, there is practically no concentration variation of components between the evaporator and film surfaces.

Figure 4 shows the effect of E_0 on the reduced distilland concentration. It is seen that, as E_0 increases, the separation becomes poorer. At higher values of E_0, therefore, large diffusional resistances cause a substantial surface depletion of Component 1, thereby lowering the separation efficiency of the still. By the same token, for $E_0 \leq 0.1$, the surface depletion of Component 1 is insignificant (Fig. 3) and the separation is very nearly the maximum attainable (Fig. 4).

Figure 5 shows the effect of the ratio of component evaporation rate coefficients on the separation efficiency of the still. As expected, the results show that, when K_f tends to unity, no fractionation of the mixture takes

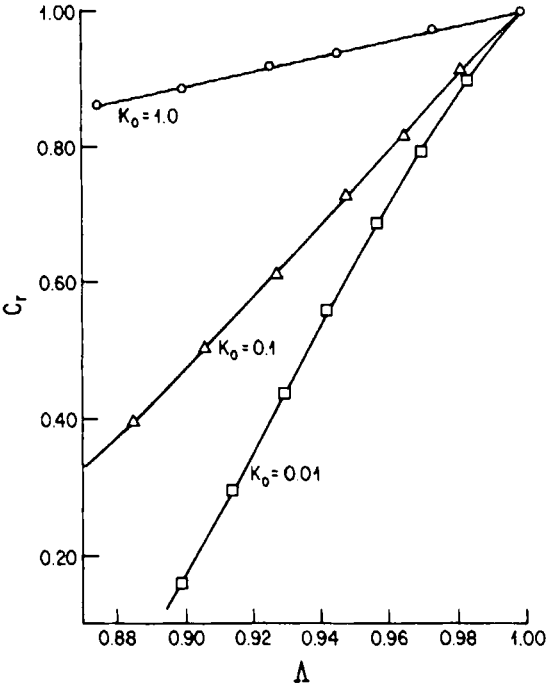

FIG. 5. Reduced film concentration of Component 1 versus Λ in falling film stills for various values of K_0, using the following values of the other parameters: $E_0 = 5.0$, $A = 15.0$, $H = 0.07$, $B - H' = 1.5$, $\gamma = 0.008$, $T'_C = 0.5$, and $C_0 = 0.25$.

place, while for low values of $K_I (K_0 \leq 0.01)$, the fractionation can be nearly completed with a single pass distillation.

The ratios of the average concentrations in the film computed for an evaporation rate controlled process and when both evaporation and diffusion play a part are plotted for various values of E_0 and K_0 in Figs. 6 and 7, respectively. From Fig. 6 it can be seen that, for $K_0 = 0.1$, the evaporation rate controlling limiting case adequately describes the falling film still if $E_0 \leq 0.1$. However, when $E_0 > 0.1$, both evaporation and diffusion affect the rate of the process. The reason for this is clear from Fig. 3, where it is seen that, for $K_0 = 0.1$ and $E_0 > 0.1$, substantial surface depletion of the lighter component begins to take place. In Fig. 7 the interfacial values of the ratio of evaporation rate coefficients (K_I) at $x = 0$, for $K_0 = 1.0$, 0.1, and 0.01, are 0.52, 0.086, and 0.008 respectively. This figure indicates that, if $K_I > 0.4$, the evaporation rate controlling approximation is still valid till $E_0 = 5$ (or $E_I \approx 1.5$).

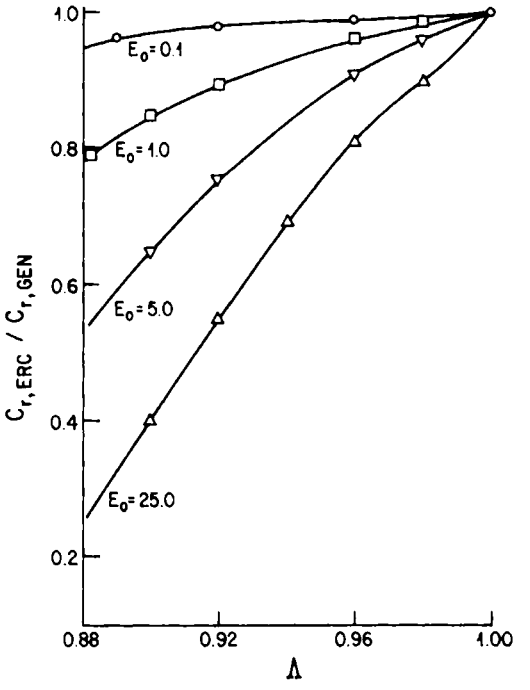

FIG. 6. Ratio of reduced film concentrations of Component 1 (evaporation rate controlling approximation to the general solutions) versus Λ in falling film stills for various values of E_0. The values of the other parameters used are the same as in Fig. 2, except that $C_0 = 0.25$ in this case.

To summarize, the evaporation rate controlling approximation can be used to describe the falling film still when at $x = 0$, E_1 ($\approx E_0$) < 0.1 for all values of $K_I > 0.086$ (or $K_0 > 0.1$); when $K_I > 0.4$, the approximation is valid for all values of $E_I < 1.5$.

Since the response of the falling film still was similar for both the constant evaporator heat flux and constant evaporator temperature cases, the results for the former are not presented.

Rotary Cone Stills—Constant Evaporator Heat Flux

The constant evaporator heat flux case was chosen since most rotary cone molecular stills use either "*in situ*" or "radiant" electrical heaters.

Due to the very thin films encountered in the rotary cone stills, it is

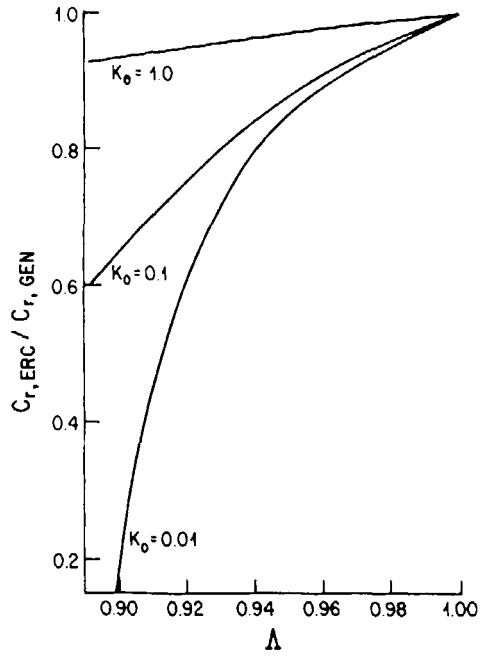

FIG. 7. Ratio of reduced film concentrations of Component 1 (ERC/general) versus Λ in falling film stills for values of K_0. The other parameters used have the same values as in Fig. 5.

expected that diffusion will not affect the rate of molecular distillation in these stills.

For the rotary cone stills it was found that neither the angular velocity of the cone nor the heat input to the still affected the surface depletion of Component 1. On the other hand, the ratio of the evaporation rate coefficients (K_1) affected the film concentration profile as shown in Figs. 8 and 9. However, Fig. 8 shows that, even for large differences in the ratio of the evaporation rate coefficients ($K_0 = 0.1$), the surface depletion of components is very low in these stills. Figure 9 shows that the separation becomes poorer as K_0 increases.

The limiting case of an evaporation rate controlled process was compared with the general solution by varying the parameters E_1, K_1, and Q. Figures 10 and 11 show the comparison. It can be seen that the concentration profiles for the two cases are nearly indistinguishable and, therefore, the distillation in these stills can be said to be an evaporation rate controlled process.

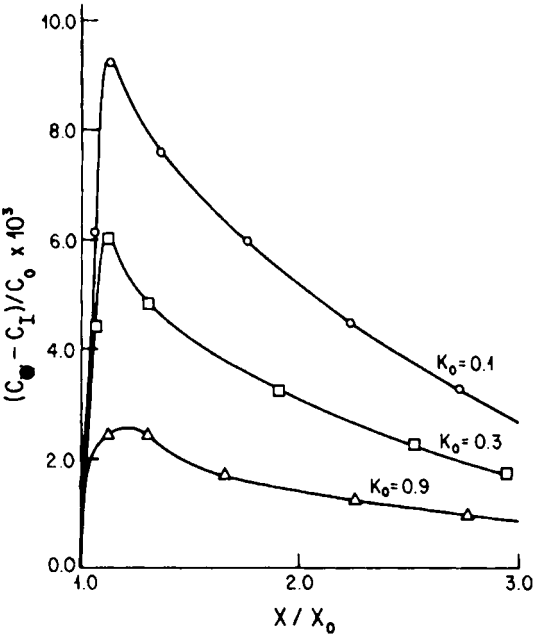

FIG. 8. Ratio of concentration differences across the film to initial concentration of Component 1 versus X/X_0 in the rotary cone stills for various values of K_0. The following values were used for the parameters involved in this plot: $E_0 = 0.05$, $A = 15.0$, $B = H' = 1.5$, $T'_C = 0.625$, $\varepsilon = 0.01$, $C_0 = 0.25$, $W = 0.5$, and $Q = 0.02$.

CONCLUSIONS

An analysis of the effect of diffusion on the molecular distillation of ideal binary liquid mixtures in the falling film and rotary cone stills led to some generalizations and conclusions, summarized as follows.

Falling Film Stills

For the falling film stills, the interaction of diffusion within the liquid film and surface evaporation has a great bearing on the separation efficiency of the still. The relative importance of diffusion and evaporation can be seen from the effect of the dimensionless parameters $E_1 = k_1\delta_0/D$ and $K_1 = k_2/k_1$. An evaporation rate controlling approximation can be used to describe the falling film still when, at the inlet of the still ($x = 0$), the dimensionless

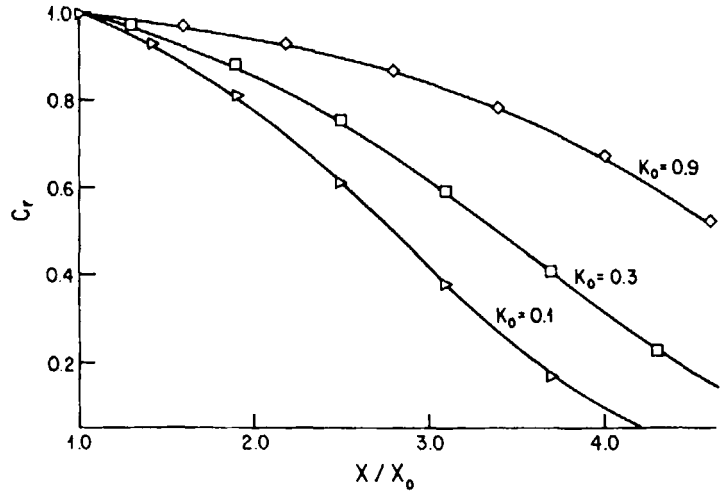

FIG. 9. Reduced film concentration (Eq. 31) versus X/X_0 for the rotary cone stills for various values of K_0. The values of the other parameters are the same as in Fig. 8.

ratio of the rates of evaporation to diffusion (E_l) is less than 0.1 for all values of the ratio of evaporation rate coefficients (K_l) greater than 0.086. When $K_l > 0.4$, this approximation is valid for all values of $E_l < 1.5$.

Rotary Cone Stills

Diffusion has no effect on the performance of these stills, as revealed by the accuracy of the evaporation rate controlling limiting solution in describing the rotary cone stills, over a wide range of distillation parameters investigated.

SYMBOLS

A	dimensionless number: b_1/T_W for the constant evaporator temperature case and b_1/T_0 for the constant evaporator heat flux case
a_i	component vapor pressure coefficient (Eq. 15)
B	dimensionless number, b_2/b_1
b_i	component vapor pressure coefficient (Eq. 15)
C	dimensionless concentration, c_1/c_T
c_i	component molar concentration (g·mol/cm^3)

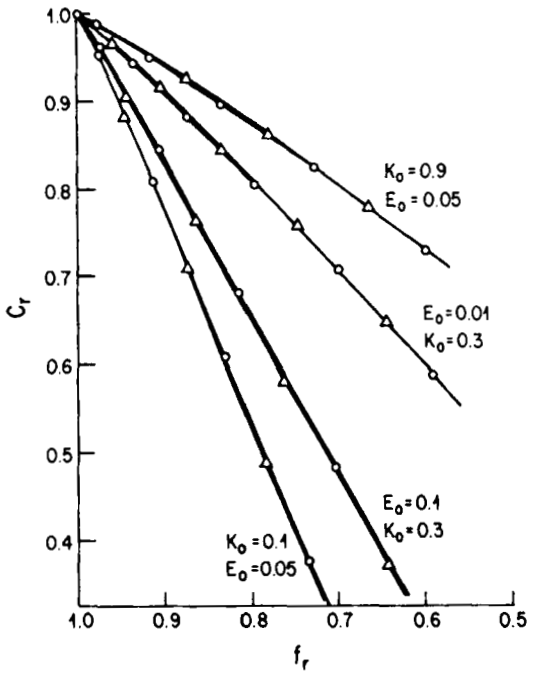

FIG. 10. Comparison of the reduced film concentration profiles of the rotary cone still general solution and evaporation rate controlling approximation for various values of E_0 and K_0. Circles represent the general solution and triangles represent the evaporation rate controlling approximation. The values of the other parameters are the same as in Fig. 9.

C_r reduced distilland concentration of component 1
D diffusion coefficient Component 1 in distilland (cm^2/s)
E dimensionless number, $k_1\delta_0/D$
f_r reduced distilland flow rate
g gravitational acceleration (980 cm/s^2)
H dimensionless number, $Dc_T\Delta h_1/\theta T_W$
H' dimensionless number, $\Delta h_2/\Delta h_1$
Δh_i component heat of vaporization (cal/g·mol)
K dimensionless number, k_2/k_1
k_i component evaporation rate coefficient (cm/s)
M_i component molecular weight (g/g·mol)
N molar vaporization rate per unit area (g·mol/cm^2·s)
P_i component vapor pressure (g/cm^2)
Q dimensionless number, $q\delta_0/Dc_T\Delta h_1$
q still heat input per unit evaporator area (cal/cm^2·s)

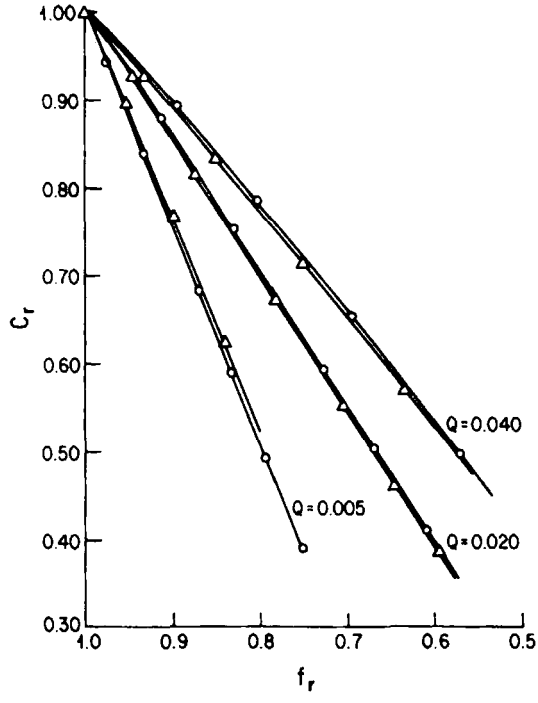

FIG. 11. Comparison of the reduced film concentration profiles of the rotary cone still general solution and evaporation rate controlling approximation for various values of Q. Circles and triangles represent the points for the general solution and evaporation rate controlling approximation, respectively. The parameters used had the same values as in Fig. 10, except that $E_0 = 0.05$, $K_0 = 0.3$, and Q varies.

R_C	radius of curvature of the falling film still evaporator (cm)
R_g	gas constant (g·cm/g·mol·°K)
T'	dimensionless temperature: T/T_W for the constant evaporator temperature case and T/T_0 for the constant evaporator heat flux case
T	absolute temperature (°K)
u	film velocity component in the x direction (cm/s)
v	film velocity component in the y direction (cm/s)
W	dimensionless number, $\omega^2 \delta_0^2 \sin^2 \phi/\nu D$
X	dimensionless number, $x\nu D/g\delta_0^4$
$\bar{X}$	dimensionless number, x/x_0
x	axial position on the still
y	distance from the evaporator surface
Y	dimensionless number, y/δ_0

Subscripts

C	condenser
d	distillate
I	film surface
0	initial condition ($x = 0$, $y = 0$)
W	evaporator surface
T	total mixture
ERC	evaporation rate controlling approximation
GEN	general solution (when both evaporation and diffusion affect the process)

Greek Letters

α	evaporation coefficient
β	dimensionless number, $\Lambda^2 d\Lambda/dx$
γ	dimensionless number, $\sigma\delta_0 T_W^3/\theta$
δ	film thickness (cm)
ε	dimensionless number, $\sigma\delta_0 T_0^4/DC_T\Delta h_1$
θ	distilland thermal conductivity (cal/cm·s·°K)
Λ	dimensionless number, δ/δ_0
μ	distilland viscosity (g/cm·s)
ν	distilland kinematic viscosity (cm^2/s)
σ	Stefan Boltzman constant
ϕ	angle substended by the evaporator surface and the cone bi-sector
ω	radial velocity of the cone (rad/s)

REFERENCES

1. Alty, T., *Philos. Mag., 15*, 82 (1933).
2. Delaney, L. J., Houston, R. W., and Eagleton, L. C., *Chem. Eng. Sci., 19*, 105 (1964).
3. Emslie, A. G., Bonner, F. T., and Peck, L. G., *J. Appl. Phys., 25*, 858 (1958).
4. Greenberg, D. B., *AIChE J., 18*, 269 (1972).
5. Hickman, K. C. D., *Nature, 88*, 881 (1936).
6. Langmuir, I., *Phys. Rev., 8*, 149 (1916).
7. Nabavian, K., and Bromley, L. A., *Chem. Eng. Sci., 18*, 651 (1963).
8. Trevoy, D. J., *Ind. Eng. Chem., 45*, 2366 (1953).
9. Watt, P. R., *Molecular Stills*, Reinhold, New York, 1960.

Received by editor December 10, 1982